

# LINEAR ACTUATOR OF THRUST VECTORING CONTROL ON SOLID ROCKET MOTOR ON LAPAN SOUNDING ROCKET

Oka Sudiana<sup>1</sup>, Khaula Nurul Hakim<sup>2</sup>

<sup>1</sup>Research Organization for Aeronautics and Space – BRIN

<sup>2</sup>Research Organization for Electronics and Informatics – BRIN

Email address of corresponding author: [oka.sudiana@brin.go.id](mailto:oka.sudiana@brin.go.id)

## ABSTRACT

Rocket Technology Center of BRIN developed a rocket with a caliber of 450 mm with passive stability using four fins on tail. The next stage, Rocket Technology Center of BRIN designed a 450mm sounding rocket with canard fin control devices as active control on the rocket. In this paper, the thrust vector control (TVC) as an alternative control device is used. The TVC has been used since it has small thrust loss and large control torque. The linear actuator of the TVC on the Solid Rocket Motor (SRM) is studied. the linear actuator of the TVC is analyzed to understanding the behavior of the thrust vector control TVC movement during flight. The simulation shown that tuning the gain of the proportional-derivative controller generate variation the control of swing nozzle movement to get desire pitch angle. The result indicates the small control of TVC nozzle movement can produce pitch angle of rocket.

© 2022 ICECREAM. All rights reserved.

Keywords: Sounding Rocket, Thrust Vector Control, Solid Rocket Motor, Linear Actuator

## 1. Introduction

The Research Center for Rocket technology-BRIN provides benefits in mastering and developing the key technologies of the rocket, including lightweight structural materials, propulsion, rocket engines, rocket flight control systems and avionics, separation systems, rocket ground systems, for scientific and military use. A rocket development program for Ground-to-Ground defense with code name is RHAN 450, has been started since 2013 through collaboration between The Research Center for Rocket technology-BRIN (formerly LAPAN) and the Ministry of Defense in collaboration with industries including PT PINDAD and PT DAHANA. Bagus [1] described that The RHAN 450 rocket has a baseline design from the 450 mm caliber Sonda

rocket RX 450 rocket (fig. 1). Bagus [1] also explained this sounding rocket is expected to be able to fly as range approximately 100 km with a potential rocket payload at least 100 kg.



Figure 1. Technical Drawing of LAPAN RX450  
Source: (Bagus, H.J., 2020)

The following are the technical specifications of the RHAN 450 for Ground-to-Ground defense rocket taken from Hakiki and Ahmad Riyadl[2]. the RHAN 450 has thrust slightly more than  $10 \times 10^3 \text{ kgf}$  from data acquisition of ground test and has its trust approximately  $10 \times 10^3 \text{ kgf}$  from sensor which is embedded in

rocket during flight. Result from Hakiki and Ahmad Riyadl[2] showed the comparison of thrust profile from static test and flight test that can be seen in fig. 2.

Table 1. Specification of RX450

1	Total length	7200 mm
2	Diameter	460 mm
3	Prediction of range	100 km
4	Diagnostic avionic	Global Positioning Sensor, Sensor Accelerometer, Sensor Gyro, Radio Telemetry, Blade Antenna

Source: (Hakiki and Ahmad Riyadl, 2016)

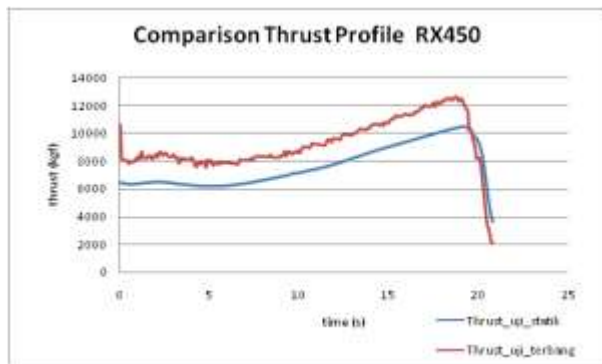


Figure 2. comparison of thrust profile during static test and flight test.

Source: (Hakiki and Ahmad Riyadl, 2016)

Rearranging the Design Requirements, Objectives, and the design of the RHAN 450 defense rocket is necessary to optimize the RHAN 450 rocket's flight. One of the improvements of its flight dynamics is by adding an active control system. There are two options for using an active control system, the aerodynamic control device (fig. 3) which was developed by lilis [3] and TVC.

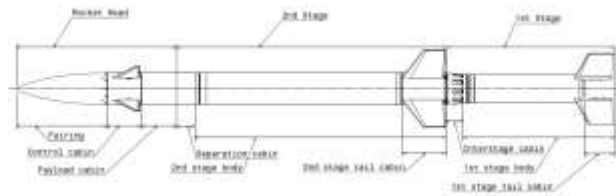


Figure 3. Concept design of dual-stage Sounding rocket RX-452

Source: (Lilis Mariani, 2020)

In this paper, the TVC as an alternative control device is used. Yeh [4] and Steer [5] discovered that the TVC technology was popularized in the development of fighter aircraft, rocket, and missile. Rocket control can benefit from TVC technology's low nozzle exit thrust loss and high control torque at a low deflection angle which mentioned by Shi et al. [6], Kutschera et al. [7], and Woodberry et al[8]. Kutschera et al. [7] given highlight the TVC several advantages of using missiles and combat aircraft. The TVC have a larger maximum Angle of Attack (AoA) and less control deflection than conventional aircraft and missiles. Woodberry et al. [8] and Ikaza [9] described the effect of the TVC, which is faster and has more controllable capabilities than the standards.

Shi et al. [6] discovered that SRM has significantly improved launch vehicle technology. Ostrander et al [10] demonstrated that the tactical missile application makes use of solid rockets because of their reliability and simplicity; utilized in a broader context for the launch of low orbit satellites; and as model rockets. In sounding rockets, thrust vector control systems are utilized to lessen the impact of perturbation. During the guidance period outlined by Wekerle et al. [11], it is able to maintain the rocket's trajectory.

The thrust vector control using solid rocket motor nozzles has been introduced with several different development methods with their own benefits. Woodberry [8] classified the

following into two main groups: the fixed-nozzle system and the movable-nozzle system. Sutton et al. [12], Prescott et al. [13], and Truchot [14] summarized the various design strategies for solid rocket motor nozzles, which can be classified into categories (fig. 4):

1. Mechanical deflection of the main nozzle; Denisikhin et al. [15] and Larkin [16] created the control forces in the rotary nozzles with rotary vectorable nozzles. A moment in relation to the rocket's mass is produced when there is an angle between the rocket's centerline and the thrust vector's direction. The absence of mechanical action on the gas jet (which results in low thrust and specific impulse losses), the linear dependence of the control force on the nozzle rotation angle, the stability of the main characteristics during SRM operation, and the relatively straightforward design are the primary advantages of rotary vectorable nozzles.
2. Insert the heat-resistant material movable parts into the exhaust jet; Recent results from Ocokoljić et al. [17], Kostić et al. [18], Ahmed et al. [19], Živković et al. [20], and Hastürk [21] imply that the jet vane control (JVC) is capable of providing the necessary roll control for missile orientation during pitch over. Roll control will keep the missile from rolling when it launches. Due to its ability to control roll, pitch, and yaw in addition to its straightforward structure, the jet vane technique is the most commonly used one.
3. Inject fluids into aside portion of the diverging nozzle section; Guo et al. [22] investigated a fluidic nozzle throat that altered the nozzle's flow area. It did not have a drive mechanism, but it was very reliable. It was also capable of integrating

direction-control and thrust-magnitude control systems.

4. Thrust-producing unit that is separate with the main propulsion system; Głębocki et al. [23] experiment using Vertical Cold Launch Missile System which was the energy to eject the missile vertically comes from some external device. Small side thrusters precisely control the projectile's attitude during the initial unpowered ascending phase of flight. Dong et al. [24] and Kang et al. [25] used A continuous type side jet controller which has four nozzles with thrust control devices was considered. It is deployed to a rocket for high maneuverability and fast controllability in the terminal guidance phase.

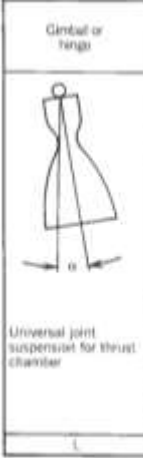
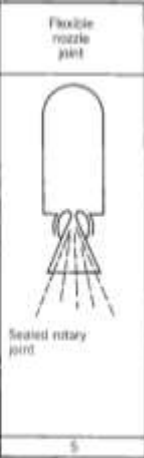
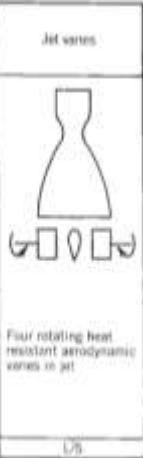
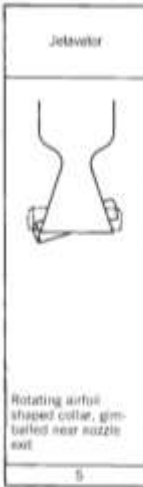
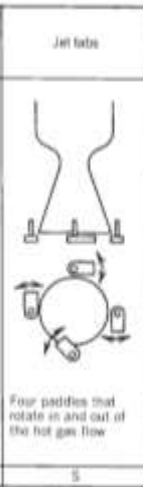
 <p>Gimbal or hinge</p> <p>Universal joint suspension for thrust chamber</p> <p>L</p>	 <p>Flexible laminated bearing</p> <p>Nozzle is held by ring of alternate layers of molded elastomer and specially formed sheet metal or plastic composite (fiberglass epoxy)</p> <p>S</p>	 <p>Flexible nozzle joint</p> <p>Sealed rotary joint</p> <p>S</p>	 <p>Jet vanes</p> <p>Four rotating heat resistant aerodynamic vanes in jet</p> <p>L/S</p>
 <p>Jetavator</p> <p>Rotating arbor shaped collar, gimbaled near nozzle exit</p> <p>S</p>	 <p>Jet tabs</p> <p>Four paddles that rotate in and out of the hot gas flow</p> <p>S</p>	 <p>Side injection</p> <p>Secondary fluid injection on one side at a time</p> <p>S/L</p>	 <p>Small control thrust chambers</p> <p>Two or more gimbaled auxiliary thrust chambers</p> <p>L</p>

Figure 4. Schematic diagrams for different TVC mechanisms. The letter L is liquid propellant rocket engines and S is solid propellant engines.  
Source: (Sutton, G. P., and Biblarz, O. 2016)

## 2. Mechanism theory and Mathematical Models

The TVC's advantages, which include low nozzle exit thrust loss and high control torque at a low angle of deflection, were outlined by Shi et al. [6], Kutschera et al. [7], and Woodberry et al [8]. The sounding rocket with nozzle movement has been utilized extensively. In both liquid and solid rocket, Thrust Vector Control (TVC) technology is currently gaining popularity. The fundamental concept of thrust vector control, as demonstrated by Catalbas and

Gulten [26], is to model the swing movement on a solid motor nozzle. This action caused the rocket to move in the desired direction. The movement of swing spout should be visible in fig.5.

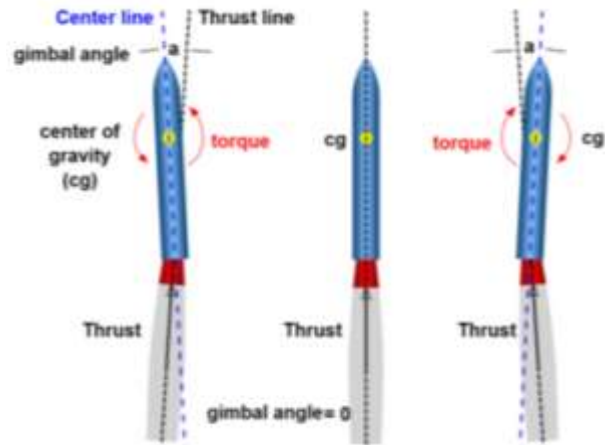


Figure 5. swing movement of nozzle effect to rocket trajectory.  
Source: (Çatalbaş, Cem and Gulten, Arif. 2017).

Movable nozzle controls the direction of the exiting flow by allowing movement of the nozzle itself. Where the flow inside the nozzle is changed following the movement of the nozzle. Its concept can be seen in fig. 6.  $\delta_p$  is the motion angle of nozzle to pitching movement and  $\delta_y$  is the motion angle of nozzle to yawing movement.

From the swing nozzle movement, thrust from nozzle and torque of rocket are generated. Were, Thrust of TVC

$$\hat{T} = \cos\delta_p \cos\delta_y \hat{x}_b + \sin\delta_y \hat{y}_b - \sin\delta_p \cos\delta_y \hat{z}_b \quad (1)$$

And torque of rocket

$$\hat{M}_T = -dT_j \hat{x}_b - l_t T \sin\delta_y \hat{y}_b - l_t T \sin\delta_p \cos\delta_y \hat{z}_b \quad (2)$$

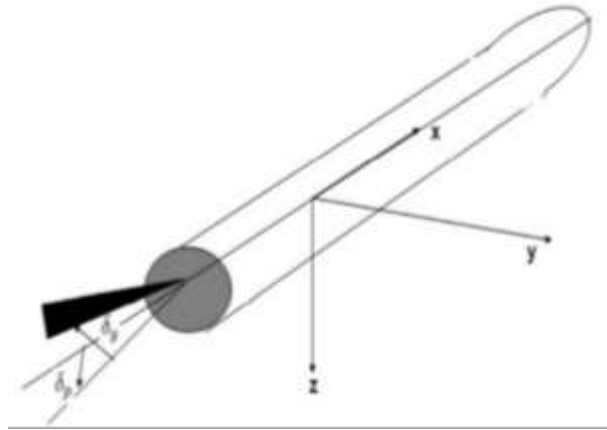


Figure 6. The angles of swing nozzle

Shelan et al. [27] and Muniraj et al. [28] stated that the PID controller is a common type of control strategy due to its ease of implementation, ability to reduce steady-state error, and ease of use. The continuous control signal  $u(t)$  of the PID controller is given by

$$u(t) = K_p e(t) + \left(\frac{1}{T_i}\right) \int e(t) dt + T(d) \quad (3)$$

from equation (1) and (2),  $\delta$  is the deflection of TVC nozzle with respect to the body of rocket. This deflection is controlled by PD controller which is given by

$$\delta = K_1 \dot{\theta} + K_2(\theta_c - \theta(t)) \quad (4)$$

The pitch angle of TVC can be seen in fig. 6, where the angle is from the deviation of the normal line angle of TVC to current position of TVC. The torsional moment due to the rotational movement of the TVC on the body rocket is shown in equation (5). Where  $M_y$  is the pitch torsion moment of the TVC,  $l$  is the distance from the rotation point of the TVC to the end of the nozzle, and  $T$  is current thrust.

Actuator control:

$$M_y = T \cdot l \cdot \sin \delta_p \quad (5)$$

$$\tan \delta_p = \frac{\Delta}{b} \quad (6)$$

$$y_c = \Delta \quad (7)$$

The linear actuator system that embedded in the TVC system can be seen in fig. 7. where the linear actuator has its own dynamics which is shown in equation (8-10).

The linear actuator dynamics:

$$m\ddot{y} + c\dot{y} + ky = F \quad (8)$$

If  $\dot{y} = V_y$  and  $\ddot{y} = \dot{V}_y$

$$\dot{V}_y = \frac{F - ky - cV_y}{m} \quad (9)$$

Where

$$F = k_p'(y - y_c) \quad (10)$$

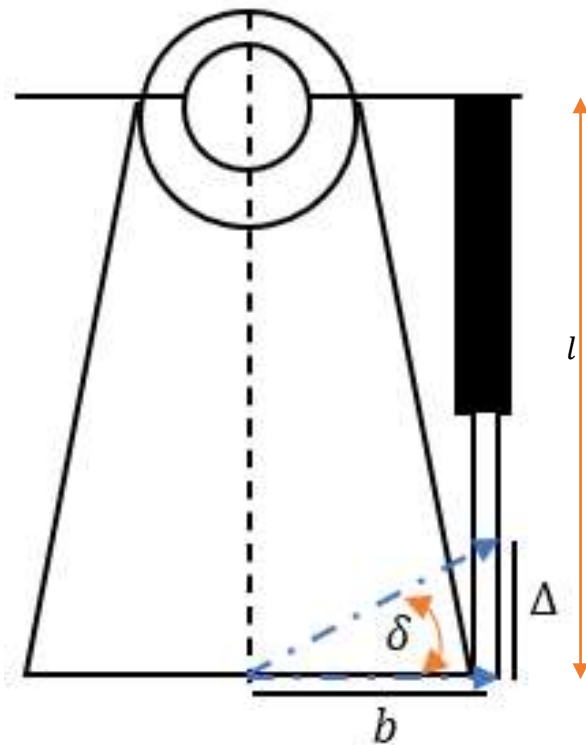


Figure 7. Linear actuator of TVC on Solid Rocket Motor concept and scheme

### 3. Result and Analysis

For this study, the following data of the Scout launch vehicle is given for determine the proportional-derivative TVC control law to implement the pitch angle from  $\theta_0 = 90^\circ$  to desired angle  $\theta_{desired} = 70^\circ$  at the end of the pith.

Table 2. characteristic of the scout launch vehicle

Total mass	:	$m_0$	=	21,643 kg
Propellant mass	:	$m_p$	=	12,810 kg
Burning time	:	$t_b$	=	70 s
Moment of inertia Y-axis	:	$I_{y_0}$	=	$7.09 \times 10^{+5}$
Specific impulse	:	$I_{sp}$	=	260 s
Length of CP to Nozzle: (initial)	:	$l_{t_0}$	=	7.53 m
(burn out)	:	$l_{t_e}$	=	8.16 m

Where:

Mass flow of propellant burn in Solid Rocket Motor:

$$m = \frac{m_0 - m_p}{t_b} \quad (11);$$

Moment of inertia shifting due to mass flow of propellant:

$$I_y = I_{y_0} - \frac{I_{y_0} - 5.75 \times 10^{+5}}{t_b} \cdot t \quad (12);$$

Length of CP to Nozzle shifting due to mass flow of propellant:

$$l_t = X C_0 + \frac{l_{t_e} - l_{t_0}}{t_b} \cdot t \quad (13)$$

The dynamic of rocket system is shown in fig. 8. using MATLAB/SIMULINK. The modeling simulation of the TVC dynamics control of the Solid Rocket Motor is made into 3 blocks (fig. 8).

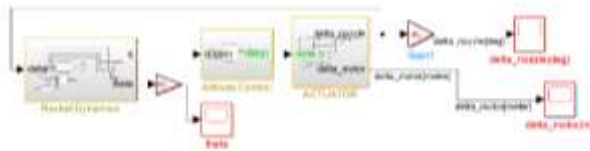


Figure 8. The longitudinal dynamics of TVC Control in sounding rocket

This division aims to facilitate the analysis of the dynamic control of the sounding rocket as a partial or full of the simulation. This is useful to check for errors and bugs clear and ease. This

simulation also used to tune proportional and derivatives of control to produce the desired output. Rocket dynamics block is used to compute the natural dynamics of the rocket. In this section, the attitude control of the rocket has not been taken to analyze the trajectory of the rocket. The output of the attitude dynamics of the rocket are the flight attitude and the trajectory of the rocket. these are used to plan the rocket flight control system.

The attitude control rocket blockset consists the proportional derivative of the flight attitude control of the rocket. This control law is given by equation (4) above.

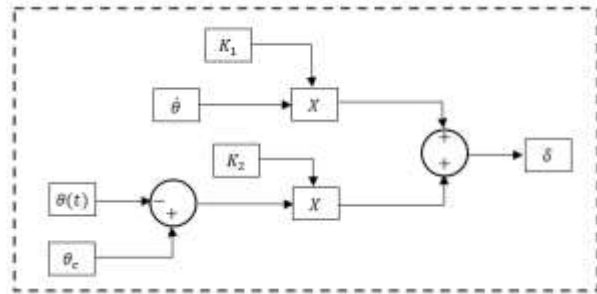


Figure 9. control law of longitudinal dynamics of TVC Control in Solid Rocket Motor

The scheme of the control law can be shown in fig. 9. The pitch rate and pitch angle are coming to TVC control of rocket blockset, then the control law generate the control of swing nozzle movement. It is to get desire pitch angle. The gains of controller are tuned to get fair performance of attitude behavior of rocket.

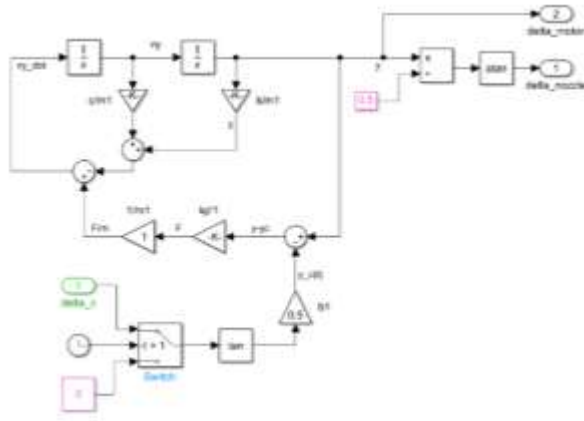


Figure 10. The schematic of the linear actuator dynamics system

The results from the simulation computations in fig. 9 produce the pitch angle ( $\delta_p$ ) of the TVC. The dynamic equation of the linear actuator is presented in the schematic which can be seen in Figure 10.

The simulation is carried out in the MATLAB/SIMULINK software. The results of the pitch angle rocket can be seen in fig. 11.

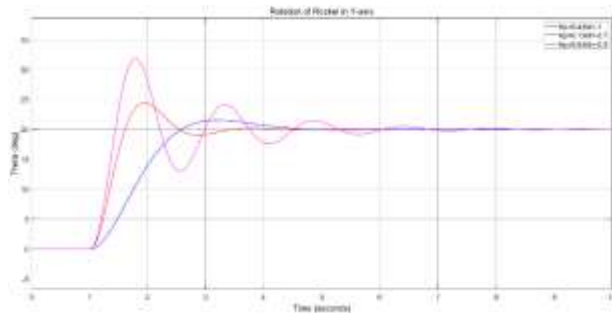


Figure 11. Rocket pitch rotation

The rocket rotates from the initial angle  $\theta_0 = 90^\circ$  to the desired angle position  $\theta_d = 70^\circ$  with a deviation angle  $\theta_c = 20^\circ$ . The control system of the rocket responds the command at the time  $t_u = 1s$ , which is the waiting time for the response from the control from the command to execution. There are some variations of PD control tuning. First tuning ( $K_p = 0.4; K_d =$

$-1$ ) has peak  $\theta_p = 24.45^\circ$  (overshoot 22.84%) at time  $t_m = 1.95s$ , with settling time The settling time of the control system from the beginning of the system response to the desired position is  $t_{set} = 5.23s$ ; meanwhile, second tuning ( $K_p = 0.1; K_d = -0.7$ ) has peak  $\theta_p = 21.51^\circ$  (overshoot 8.15%) at time  $t_m = 3.20s$ , with settling time is  $t_{set} = 6.78s$ ; and the last tuning ( $K_p = 0.5; K_d = -0.5$ ) has peak  $\theta_p = 31.82^\circ$  (overshoot 60.48%) at time  $t_m = 1.80s$ , with settling time is  $t_{set} = 9.88s$ .

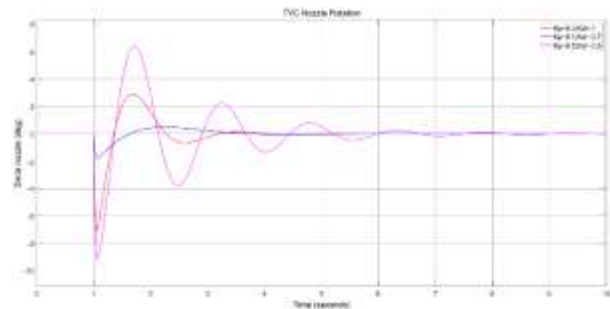


Figure 12. TVC Nozzle Rotation

Figure 12 represents a rotating TVC Nozzle. TVC Nozzle receives response from the linear actuator to rotate the direction of the thrust flow coming out of the nozzle. These effect changes the rocket's attitude position so that the rocket rotates to the desired position. At first tuning, TVC nozzle rotates  $\delta_p = 7.07^\circ$  to push the rocket rotates on the y-axis to the desired position. To counter the overshoot from the desired position of the rocket, the TVC Nozzle rotates in the opposite direction. It has 2 cycles until the system stable. Second tuning has  $\delta_p = 1.82^\circ$  and only has a cycle to stabilize the system; and the last one has  $\delta_p = 9.20^\circ$  and has over 6 cycles until the system stable.

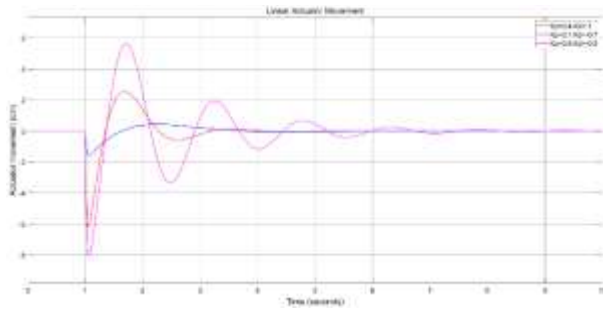


Figure 13. Linear Actuator movement

TVC Nozzle rotates due to the push and retract of the actuator linear drive rod. Linear Actuator responds commands from the control system which can be seen in Figure 13. The result of the simulation, at first tuning, the linear Actuator retracts the driving rod with maximum  $\Delta = 6.20\text{cm}$  to rotate the TVC nozzle. While, from second tuning given a maximum retract  $\Delta = 1.58\text{cm}$ ; and the last tuning has a maximum retract  $\Delta = 8.10\text{cm}$

Table 2. Comparisons of TVC system dynamics

	Kp	Kd	Peak	Tm [s]	Overshoot [%]	Ts [s]
Rotation rocket in Y-axis	0.4	-1	24.4 [deg]	1.9	22.8	5.2
	0.1	-0.7	21.5 [deg]	3.2	8.1	6.7
	0.5	-0.5	31.8 [deg]	1.8	60.4	9.8
TVC Nozzle Rotation	0.4	-1	7.0 [deg]	1.0	42.1	4.0
	0.1	-0.7	1.8 [deg]	1.0	27.5	3.7
	0.5	-0.5	9.2 [deg]	1.0	110.8	9.6
Linear actuator movement	0.4	-1	6.2 [cm]	1.0	42.1	4.0
	0.1	-0.7	1.5 [cm]	1.0	27.5	3.7
	0.5	-0.5	8.1 [cm]	1.0	114.1	9.6

#### 4. Conclusions

The paper provides TVC system scheme with a SRM nozzle is driven by linear actuator. The entire actuation system, which has been modeled in MATLAB/SIMULINK to confirm the results of simulations of the proposed system. This simulation can well represent the

attitude behavior of TVC nozzle. From the simulation can be seen that tuning the gain of the proportional-derivative controller generate variation the control of swing nozzle movement to get desire pitch angle. The result indicates the small control of TVC nozzle movement can produce pitch angle of rocket.

#### Acknowledgements

Foremost, we would like to express our sincere gratitude to Stefano Carletta, PhD, for his patience, drive, enthusiasm, and vast knowledge, as well as his ongoing support of the research. Special thanks addressed to BRIN (formerly Kemenristekdikti) through RisetPRO Non-Degree program for financial support in doing this research. And also, to Research Center of Rocket Technology-BRIN Indonesia which has support for my research, which is very useful for completing the research.

#### References

- [1] Bagus, H.J. (2020). *Program Manual Kerekayasaan Pengembangan Teknologi Roket Tahun 2020*. Pusat Teknologi Roket. LAPAN
- [2] Hakiki and Ahmad Riyadl. (2016). *Analisis kestabilan dan prestasi terbang RX-450 berdasarkan hasil uji terbang*. Seminar Nasional IPTEK Penerbangan dan Antariksa XX-2016
- [3] Lilis Mariani. (2020). *Dissemination technology of two-stage sonda rocket for development military rocket rhan 450 with range 100 km*. National research priority.
- [4] F. K. Yeh. (2012). *Adaptive-sliding-mode guidance law design for missiles with thrust vector control and divert control system*. Control Theory and Applications Iet, vol. 6, no. 4, pp. 552–559.
- [5] Steer. (2000). *Integrated control of a second-generation supersonic commercial transport aircraft using thrust vectoring*. ser. Guidance, Navigation, and Control and Co-located

- Conferences. American Institute of Aeronautics and Astronautics.
- [6] Shi, C., Yang, J., & Xu, Z. (2020). *Research on thrust vector control of nonlinear solid rocket motor nozzle based on active disturbance rejection technology*. In MATEC Web of Conferences (Vol. 309, p. 04008). EDP Sciences.
- [7] Kutschera, A., & Render, P. M. (2002). *Advanced combat aircraft performance assessment*. The Aeronautical Journal, 106(1062), 443-452.
- [8] Woodberry, R. F. H., & Zeamer, R. J. (1974). *Solid rocket thrust vector control*. NASA SP-8114, 4-17.
- [9] Ikaza, D. (2000). *Thrust vectoring nozzle for modern military aircraft*. INDUSTRIA DE TURBO PROPULSORES MADRID (SPAIN).
- [10] Ostrander, M., Bergmans, J., Thomas, M., & Burroughs, S. (2000). *Pintle motor challenges for tactical missiles*. In 36th AIAA/ASME/SAE/ASEE Joint Propulsion Conference and Exhibit (p. 3310).
- [11] Wekerle, T., Barbosa, E. G., Batagini, C. M., da Costa, L. E. L., & Trabasso, L. G. (2016). *Closed-loop actuator identification for Brazilian Thrust Vector Control development*. IFAC-PapersOnLine, 49(17), 468-473.
- [12] Sutton, G. P., & Biblarz, O. (2016). *Rocket propulsion elements*. John Wiley & Sons.
- [13] Prescott, B. H., & Macocha, M. (1996). *Nozzle design*. PROGRESS IN ASTRONAUTICS AND AERONAUTICS, 170, 137-187.
- [14] Truchot, A. (1988). *Design and Analysis of Solid Rocket Motor Nozzle*. Agard Lecture Series, (150).
- [15] Denisikhin, S., Emelyanov, V., & Volkov, K. (2021). *Fluid dynamics of thrust vectorable submerged nozzle*. Fluids, 6(8), 278.
- [16] Larkin, D., & Singh, H. (2011). *Thrust-Vector Control*.
- [17] Ocokoljić, G., Rašuo, B., Damljanović, D., & Živković, S. (2020). *Experimental and numerical research of the influence of thrust vector control on the missile aerodynamics by cold and hot jet simulations*. FME Transactions, 48(4), 770-778.
- [18] Kostić, O., Stefanović, Z., & Kostić, I. (2017). *Comparative cfd analyses of a 2d supersonic nozzle flow with jet tab and jet vane*. Technical Gazette, 24(5), 1335-1344.
- [19] Ahmed, A., Baig, A., Shah, B. H., & Rafique, M. (2016, January). *Numerical study of the effect of geometric parameters on jet tab based TVC system*. In 2016 13th International Bhurban Conference on Applied Sciences and Technology (IBCAST) (pp. 509-514). IEEE.
- [20] Živković, S. Ž., Milinović, M. M., Stefanović, P. L., Pavlović, P. B., & Gligorijević, N. I. (2016). *Experimental and simulation testing of thermal loading in the jet tabs of a thrust vector control system*. Thermal Science, 20, S275-S286.
- [21] Hastürk, Ö. (2015, July). *A novel electromechanical actuator for missile jet vane thrust control*. In 2015 IEEE International Conference on Advanced Intelligent Mechatronics (AIM) (pp. 1298-1302). IEEE.
- [22] Guo, C., Wei, Z., Xie, K., & Wang, N. (2017). *Thrust control by fluidic injection in solid rocket motors*. Journal of propulsion and power, 33(4), 815-829.
- [23] Głębocki, R., & Jacewicz, M. (2020). *Sensitivity analysis and flight tests results for a vertical cold launch missile system*. Aerospace, 7(12), 168.
- [24] Dong, T., Zhao, C., & Song, Z. (2019). *Autopilot Design for a Compound Control Small-Scale Solid Rocket in the Initial Stage of Launch*. International Journal of Aerospace Engineering, 2019.
- [25] Kang, K. T., Lee, E., & Lee, S. (2015). *Numerical investigation of jet interaction for missile with continuous type side jet thruster*. International Journal of Aeronautical and Space Sciences, 16(2), 148-156.

- [26] Çatalbaş, Cem and Gulten, Arif. (2017). *A Novel Approach for Optimization of Nozzle Angle and Thrust Vectoring Controller via a Sub-Mutation Genetic Algorithm*. International journal of innovative computing, information & control: IJICIC. 13. 1929–1940. 10.24507/ijicic.13.06.1929.
- [27] Shelan, Sameh Fathey, et al (2020). *FPGA-based Controller For Electro-Mechanical Fin Actuation System Using Processor In The Loop (PIL)*. 2020 12th International Conference on Electrical Engineering (ICEENG). IEEE.
- [28] Muniraj, Murali, and Ramaswamy Arulmozhiyal. (2015). *Modeling and simulation of control actuation system with fuzzy-PID logic controlled brushless motor drives for missiles glider applications*. The Scientific World Journal 2015.